# Density Functional Theory Study of Substituent Effects on the 1,3-Dipolar Cycloaddition Mechanism

Pengliag Sun[1], Meng Liu[2], Wei Pu[1], Yi Jin[1], Shixi Liu[1], Qiue Cao[1], and Zhongtao Ding[1]

[1]Yunnan University
[2]Chinese Academy of Sciences

May 29, 2020

**Abstract**

In this study, we performed density functional theory calculations using the B3LYP, M052X, M062X, and APFD functionals to investigate substituent effects on the mechanism of 1,3-dipolar cycloaddition, a classical and effective method for the synthesis of heterocyclic compounds. The results showed that changing the substituents on the chloroxime compounds affects the energy level of the highest occupied molecular orbital and consequently, the progress of the reaction. Finally, it provided an effective idea for this kind of reaction in the design of organic synthesis and the necessary theoretical basis for revealing the course of this reaction.

**Abstract**

In this study, we performed density functional theory calculations using the B3LYP, M052X, M062X, and APFD functionals to investigate substituent effects on the mechanism of 1,3-dipolar cycloaddition, a classical and effective method for the synthesis of heterocyclic compounds. The results showed that changing the substituents on the chloroxime compounds affects the energy level of the highest occupied molecular orbital and consequently, the progress of the reaction. Finally, it provided an effective idea for this kind of reaction in the design of organic synthesis and the necessary theoretical basis for revealing the course of this reaction.

**Keywords:** 1,3-dipolar cycloaddition reaction; Density functional theory; Reaction mechanism;

## Introduction

1,3-Dipolar cycloaddition is a reaction that not only plays an important role in the synthesis of five-membered heterocyclic compounds, but also has great significance in theoretical organic chemistry.[1-4] Diversity-oriented synthesis refers to a kind of forward synthesis that usually uses branching diffusion to focus on the diversity and complexity of compounds with the aim of expanding the compound library from point to face.[5-7] Because this synthetic method can use combinatorial chemistry to synthesize similar compounds, the properties and structure-activity relationship of the synthesized compounds can be easily studied.[8]Moreover, it hastens the building of a library of natural products with diverse molecular skeletons, complex structures, and rich chemical properties and facilitates the discovery of more lead compounds.[9]

To discover anti-tumor compounds with novel, molecularly diverse skeletons, several research groups have joined the field of antitumor treatment. At present, in the context of drug resistance, the use of the 1,2,4-oxadiazole skeleton has become a new direction in drug design.[10-13] Among the compounds with this skeleton, 3-aryl-5-(3-chlorothiophene-2-yl)-1,2,4-oxadiazole compounds have exhibited good activity for a few breast and colon cancer cell lines and retained activity in experiments with mice.[14] A series of novel triaryl-1,2,4-oxadiazole derivatives synthesized by Miralinaghi et al. also showed good cytotoxic activity against the MCF-7 tumor cell line (IC50 = 6.50 μM).[15] Gakh et al. developed a series of diaryl-5-amino-1,2,4-oxadiazole

derivatives as powerful tubulin inhibitors. The 4-position PhNH fragment on the aryl group of the compound is the decisive pharmacophore of compound activity. Compounds DCP 10500071 and DCP 10500078 showed particularly good activity against tubulin with IC50 values of 2.6 and 1.9 μM, respectively.[16] Muraglia et al. developed a series of 4-(3-(quinoline-2-yl)-1,2,4-oxadiazole-5-yl) piperazine urea compounds for the treatment of tumors with abnormal Hedgehog signaling pathway. Moreover, a structure-activity relationship study confirmed that these compounds are particularly effective antagonists and show a certain antitumor activity in mice.[17] In addition, the 1,2,4-oxadiazole derivatives, BDM31343, BDM31381, and BDM41906, which were designed by structure-activity relationship analysis, were found to be useful reagents for the treatment of pulmonary tuberculosis. They have shown improved activity, through indirect in vivo experiments, and have effectively overcome the resistance of pulmonary tuberculosis to ethylthioisoamide.[18-19] In addition, a few 1,2,4-oxadiazole derivatives showed great potential in the treatment of Alzheimer's disease. Specifically, these drugs can prevent amyloid protein polymerization and related oxidative stress, resulting in neuroprotective effects.[20] Phidianidine has been synthesized and used to evaluate the neuroprotective effects of compounds on SH-SY5Y cells by introducing it simultaneously with neurotoxic substances, such as Aβ 25-35, hydrogen peroxide, and oxidized glucose. The results showed that phidianidine exhibited a good neuroprotective effect in vitro and counteracted the effects of these neurotoxic substances.[21-22] Indolone, as the main skeleton of alkaloids, has always been considered by pharmaceutical chemists, especially in the development of new therapeutic drugs.[23-25] Indolone derivatives have a good biological potential because of its various biological activities,[26] such as antibacterial, anti-tuberculosis, antioxidant, antihistamine, anti-HIV, anti-inflammatory, anti-Parkinson, anti-diabetic, and antitumor activities.[27] At present, several of these biological activities have also been well studied. Through these studies, indolone can be modified more scientifically and reasonably, and this will play a vital role in the development of effective drug therapy in the future.[28] In addition, the synthesis and properties of oxime compounds remains an important direction in pesticide research.[29] Therefore, by using the 1,3-dipolar compound, *o* -chlorobenzoxime, and compounds with both electrophilic and affinity sites, heterocyclic compounds with novel structures and natural products can be synthesized by a simple and rapid method. However, details of the 1,3-dipolar cycloaddition mechanism of substituted chloroxime compounds remains unclear because theoretical analysis of such reactions is rarely reported. In view of the current research on the 1,3-dipolar cycloaddition mechanism, the purpose of this study was to analyze the effect of substitution of chloroxime compounds by quantum chemical calculations combined with thermodynamic and kinetic studies. The effects of different substituents on the liquid- and gas-phase reaction mechanisms were explained.

In this study, the 1,3-dipolar cycloaddition product synthesized by multiple guiding methods was used as the system. Using four different density functionals, B3LYP, M052X, M062X, and APFD, the 1,3-dipolar cycloaddition mechanism was determined theoretically. In summary, we revealed the effects of different chloroxime substituents on the 1,3-dipolar cycloaddition mechanism, which are consistent with the law of organic reaction. Thus, our findings provide a theoretical explanation of experimental phenomena and guidance for the development of new processes.

**Computational Details**

In this study, geometry optimization and vibrational analysis of a series of reactants, products, intermediates, and transition states were carried out using the 6-31G(d) basis set and B3LYP, M052X, M062X, and APFD functionals. The calculated results were analyzed, and the similarities and differences between these functionals were determined. Studies of the reaction mechanism in the solution and gas phases and the search for the transition states were performed using the Gaussian 09W D.01 9.0 program.[30] Configuration optimization of the reactants, products, intermediates, and transition states was carried out at the B3LYP/6-31G(d) level. The reaction mechanism in solution was calculated at the B3LYP/6-31G(d) level using the intrinsic reaction coordinate (IRC) and polarizable continuum model (PCM) methods. The curves of the bond angle, bond length and energy of the transition state with the reaction coordinates are obtained. The vibrational states of the optimized transition states, TS1–TS3, were analyzed to determine whether the force constant matrix only has one negative eigenvalue and confirm the authenticity of the transition state. The vibration mode corresponding to the eigenvector pointed to the corresponding reactants and products in the reaction.

And we used GaussView 5.0 to view the frontier orbitals of the molecules at the B3LYP/6-31G(d) level. The transition state is searched and the vibration frequency is analyzed at the M062X/6-31G(d) level, and the reaction intermediate and transition state can be determined by vibration analysis. We also carried out the (IRC) analysis of the intrinsic reaction coordinates to determine whether the transition state can truly reflect the relationship between the reactants and the products. Finally, the single-point energies of the stationary points were calculated at the MP2/cc-pVTZ level, and the relevant thermodynamic data (zero-point energy and Gibbs free energy) were obtained. The reactions of different substituted compounds and trends in the activation energies ($\Delta E_{\ a}$) during the reaction were compared and analyzed.

## Results and Discussion

In this study, we initially used substituted chloroxime (**1a** –**o** ) and isatin (**2a** –**e** ) compounds as the raw materials. As indicated in the synthetic route shown in Scheme 1, novel polyheterocyclic 1,2,4-oxadiazolindolone compounds were obtained in high yield in a one-step reaction under relatively mild reaction conditions without using any metal catalyst. A total of 36 target compounds were synthesized with yields of 46–96%. The proposed reaction mechanism is shown in Scheme 2. In addition, our research group has published our main synthetic methods and related results (for specific synthetic methods and characterization, see Supporting Information 1).[31] To deeply and systematically study the details of the 1,3-dipolar cycloaddition mechanism and effect of different substituents, we performed density functional theory calculations using various functionals.

**Scheme 1.** Synthesis of heterocyclic 1,2,4-oxadiazolindolone compounds.

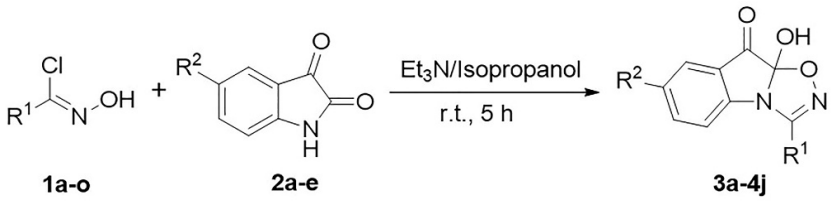


**1a-o:** $R^1$ = Ph, *p*-$CH_3C_6H_4$, *m*-$CH_3C_6H_4$, *o*-$CH_3C_6H_4$, PhEt, *p*-$OCH_3C_6H_4$, *p*-$FC_6H_4$, *m*-$FC_6H_4$, *o*-$FC_6H_4$, *p*-$ClC_6H_4$, *m*-$ClC_6H_4$, *o*-$ClC_6H_4$, Br, Thiophene, *n*-Pr

**2a-e:** $R^2$ = H, F, $OCH_3$, $CH_3$, Br

**Scheme 2.** Proposed reaction mechanism of the synthetic route.

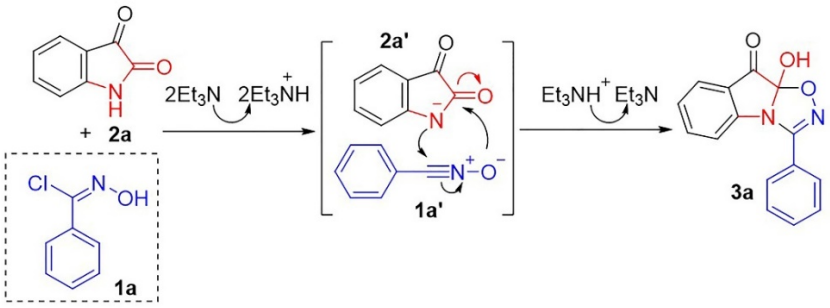


## Frontier orbital theory.

According to frontier orbital theory, similar to the valence electron interaction of a single atom, there are also valence electrons, that is, the electrons in the frontier orbitals, in a molecular reaction. During

bonding, the frontier orbital will take precedence.[32]During 1,3-dipolar cycloaddition, the H and Cl atoms leave reactant**1a** to form intermediate **1a'** , while the H atom leaves**2a** to form intermediate **2a'** , The frontier orbitals involved in cyclization are those of intermediates **1a'** and**2a'** . Therefore, we determined the frontier orbital energy difference between these intermediates. The lowest unoccupied molecular orbital 1 ($LUMO_1$)-highest occupied molecular orbital 2 ($HOMO_2$) and $LUMO_2$-$HOMO_1$energy differences between isatin substituted with -H, -F, -OCH, -$CH_3$, or -Br and chloroxime compounds with different substituents are shown in Tables 1 and Table S2.1-S2.4 of supporting information.

**Table 1.** Energy level differences between the lowest unoccupied molecular orbitals (LUMOs) and highest occupied molecular orbitals (HOMOs) of **1a'** –**1o'** and **2a'** .

| Reactant | R | LUMO | HOMO | $LUMO_1$-$HOMO_2$ | $LUMO_2$-$HOMO_1$ |
|---|---|---|---|---|---|
| 2a' | H | 0.07888 | -0.03095 | / | / |
| 1a' | Ph | -0.04827 | -0.23293 | -0.01732 | 0.31181 |
| 1b' | *p*-$CH_3C_6H_4$ | -0.04422 | -0.22678 | -0.01327 | 0.30566 |
| 1c' | *m*-$CH_3C_6H_4$ | -0.04469 | -0.23028 | -0.01374 | 0.30916 |
| 1d' | *o*-$CH_3C_6H_4$ | -0.04658 | -0.22958 | -0.01563 | 0.30846 |
| 1e' | PhEt | -0.04314 | -0.22572 | -0.01219 | 0.30460 |
| 1f' | *p*-$OCH_3C_6H_4$ | -0.04520 | -0.22807 | -0.01425 | 0.30695 |
| 1g' | *p*-$FC_6H_4$ | -0.04904 | -0.23363 | -0.01809 | 0.31251 |
| 1h' | *m*-$FC_6H_4$ | -0.05706 | -0.24011 | -0.02611 | 0.31899 |
| 1i' | *o*-$FC_6H_4$ | -0.05488 | -0.23648 | -0.02393 | 0.31536 |
| 1j' | *p*-$ClC_6H_4$ | -0.05932 | -0.23764 | -0.02837 | 0.31652 |
| 1k' | *m*-$ClC_6H_4$ | -0.06043 | -0.24262 | -0.02948 | 0.32150 |
| 1l' | *o*-$ClC_6H_4$ | -0.05903 | -0.23913 | -0.02808 | 0.31801 |
| 1m' | *p*-$BrC_6H_4$ | -0.05962 | -0.23642 | -0.02867 | 0.31530 |
| 1n' | Thiophene | -0.04608 | -0.23110 | -0.01513 | 0.30998 |
| 1o' | n-Pr | -0.03354 | -0.24335 | -0.00259 | 0.32223 |

1,3 Dipolar cycloaddition reactions can be divided into three types: (1) those with the LUMO provided by the 1,3-dipole are collectively called LUMO-controlled reaction, (2) those with the HOMO provided by the 1,3-dipole are collectively called HOMO-controlled reaction, and (3) those wherein both of the above conditions occur are collectively called LUMO-HOMO controlled reaction. As can be seen in Tables 1, $LUMO_1$-$HOMO_2$ < $LUMO_2$-$HUMO_1$; therefore, 1,3-dipolar cycloaddition requires symmetry matching between the LUMO of the substituted chloroxime, which acts as the electron acceptor, and HOMO of the substituted isatin, which acts as the electron donor. The interaction between the two compounds leads to the formation of a σ bond, which reduces the energy of the system. Because the 1,3-dipole provides the LUMO for a LUMO-controlled reaction, a lower LUMO energy level for the chloroxime compound is more conducive to the reaction. Analysis of the data in Tables 1 and Table S2.1-S2.4 indicates that the LUMO energy levels of the substituted compounds increase in the order Ph < thiophene < n-Pr. Therefore, the LUMOs of phenyl-substituted compounds are more conducive to the progress of the reaction, which is consistent with the experimental results (For experimental data, see table1 and table S1).

When the chloroxime compound contains a substituted phenyl group, the LUMO energy level increases in the order Br < Cl < F < H < $OCH_3$ < $CH_3$ < Et, while the degree of difficulty of the reaction decreases in the order Br > Cl > F > H > $OCH_3$ > $CH_3$ > Et. According to the general law of organic pericyclic reactions, an electron-withdrawing group reduces the LUMO energy level of the dienophile. A 1,3-dipole substituted with an electron-withdrawing group has a lower LUMO energy level, which is consistent with the calculated results. Among the electron-withdrawing groups, F, Cl and Br were used to reduce the LUMO energy level of the reactant. On the other hand, the electron-donating groups $OCH_3$, $CH_3$, and Et increase the LUMO energy level of the reactant. F has a stronger electron-withdrawing effect than Cl and

Br. However, in the 1,3-dipole, the 2p orbital electron of F is conjugated to the benzene ring because being in the same period, F and C have a similar 2p orbital radius. Consequently, the two orbitals can overlap better, which strengthens conjugation but weakens the induced electron-withdrawing ability of F. However, when the conjugate electron donor and induced electron-withdrawing abilities are combined, the latter is still exhibited by the F substituent.

When the substituent is a halogen, substitution at the meta position leads to a lower LUMO energy level, which is more conducive to the reaction, compared with substitution at the ortho or para position. When the substituent is an alkyl group, the LUMO energy level increases in the order ortho < meta < para, that is, having an ortho substituent is more conducive to the reaction. However, increasing the length of the alkyl chain increases the LUMO energy level, which is not conducive to the reaction.

In this reaction system, isatin provides the HOMO. Analysis of the theoretical data indicates that the HOMO energy levels of the different substituted compounds increase in the order Br < F < $OCH_3$ < H < $CH_3$. According to the general law of organic pericyclic reactions, an electron-donating group increases the HOMO energy level of dienes. Isatin compounds substituted with such a group have a higher HOMO energy level, which is in good agreement with the above calculated results. In addition, the energy level difference between $LUMO_1$ and $HOMO_2$ also reflects the degree of difficulty of the reaction to a certain extent. However, in the actual reaction, the degree of difficulty also depends on other factors, such as steric hindrance and symmetry matching of the orbitals.

Subsequently, we calculated the LUMO and HOMO energy levels of intermediates **1a'** and **2a'** using the 6-31G(d) basis set and M052X, M062X, and APFD functionals (see Supporting Information 2 for details). The results are in good agreement with the above conclusions, although there are a few differences in the relative numerical value, which is within the range of experimental error. The values calculated using the APFD functional are similar to those calculated using the B3LYP functional; however, those calculated using M052X and M062X functionals are different. This is mainly reflected in the higher LUMO energy level and lower HOMO energy level. Because there is no reference value for comparison, it is impossible to determine which functional is more suitable for calculations for this system. In terms of time consumption, using the same calculation parameters for the same compound, the functionals that are similar are B3LYP and APFD and M052X and M062X. However, the computing times using M052X and M062X are about twice as long as that using B3LYP. In summary, the conclusions obtained from the calculations of the frontier orbital energies for this system using the four functionals are completely consistent. Therefore, B3LYP is more economical and efficient for batch calculation of these compounds.

Finally, at the B3LYP/6-31G(d) level, we used PCM with triethylamine as the solvent to calculate the frontier orbital energy difference between**1a'** and **2a'** , and the results are shown in Table S2.5-S2.8 of supporting information. Analysis of the data shows that the substituent effect is completely consistent with that in the gas phase. This proves that the use of triethylamine as the solvent only has a minor effect on the reaction. Specifically, the energy level difference for **1a'** in the solvent phase is basically close to that in the gas phase. However, owing to the induced electron-withdrawing ability of triethylamine, the calculated LUMO and HOMO energy levels of**2a'** are slightly lower.

### Γιββς φρεε ενεργψ (ΔΓ).

The ΔG of each reaction was calculated at the B3LYP/6-31G(d) level, as shown in Table 2. The magnitude of ΔG can be used to predict the difficulty or ease of the reaction. Among the phenyl, thiophene, and alkyl substituents, the phenyl group is the most favorable for the reaction. On the other hand, the alkyl group is not conducive to reaction progress, which is consistent with experimental data and the conclusion derived from frontier orbital theory discussed in section 3.1. For chloroxime compounds containing a substituted phenyl group, the ΔG and hence, difficulty, of the reaction, decreases in the order Et > H > $OCH_3$ > F > Cl > Br. Moreover, the effect of an ortho substituent is stronger than those of meta and para substituents, which basically agrees with the relevant law of organic reaction.

The M052X, M062X, and APFD functionals were also used to calculate the ΔG of the 36 reactions (see

Supporting Information 3 for details). The ΔG values obtained using these three functionals are negative, indicating that the reactions can occur in the standard gaseous state. The APFD functional takes less computing time, although the ΔG regularity of each reaction is small. M052X and M062X calculations are time consuming and yield similar ΔG values that are basically consistent with the general law of organic reaction. For substituted **1a**reactants, the ΔG and hence, difficulty, of the reaction increases in the order Ph < thiophene < n-Pr. For chloroxime compounds containing a halogen-substituted phenyl group, the ΔG of the reaction is lower, that is, substitution with F, Cl, Br, or other halides is more conducive to the reaction. The effect is strongest when the substituent is in the ortho position. For reactant **2a** , substitution with $OCH_3$ or other electron-donating groups is more conducive to the reaction. It can be concluded that if**1a** contains an electron-withdrawing group, an electron-donating group on **2a** is more conducive to the reaction. According to the above analysis, the ΔG values calculated using B3LYP, M052X, and M062X are basically consistent with the general law of organic reaction.

**Table 2.** ΔG of the reactions under gas-phase condition.

| Reaction | Product | ΔG (kcal·mol$^{-1}$) | Reaction | Product | ΔG (kcal·mol$^{-1}$) |
|---|---|---|---|---|---|
| 1a+2a | **3a** | 0.60 | **1g+2b** | **3s** | 0.47 |
| 1b+2a | **3b** | -1.17 | **1a+2c** | **3t** | -0.53 |
| 1c+2a | **3c** | 0.55 | **1b+2c** | **3u** | -2.16 |
| 1d+2a | **3d** | -2.13 | **1d+2c** | **3v** | -3.12 |
| 1e+2a | **3e** | 0.68 | **1g+2c** | **3w** | -0.48 |
| 1f+2a | **3f** | -0.83 | **1i+2c** | **3x** | -3.70 |
| 1g+2a | **3g** | 0.67 | **1a+2d** | **3y** | 0.64 |
| 1h+2a | **3h** | 0.45 | **1b+2d** | **3z** | -0.48 |
| 1i+2a | **3i** | -2.52 | **1d+2d** | **4a** | -2.18 |
| 1j+2a | **3j** | 0.54 | **1g+2d** | **4b** | 0.70 |
| 1k+2a | **3k** | 0.59 | **1h+2d** | **4c** | 0.38 |
| 1l+2a | **3l** | -0.53 | **1i+2d** | **4d** | -2.56 |
| 1m+2a | **3m** | 0.50 | **1j+2d** | **4e** | 0.58 |
| 1n+2a | **3n** | 0.14 | **1a+2e** | **4f** | 0.50 |
| 1o+2a | **3o** | 1.51 | **1b+2e** | **4g** | -0.43 |
| 1a+2b | **3p** | 0.35 | **1d+2e** | **4h** | -2.26 |
| 1b+2b | **3q** | -0.91 | **1g+2e** | **4i** | 0.70 |
| 1f+2b | **3r** | -1.20 | **1j+2e** | **4j** | 0.63 |

The ΔG values were also calculated at the B3LYP/6-31G(d) level using PCM with triethylamine as the solvent, and the results are shown in supporting information 3.1. The ΔG values of the reactions are negative, indicating that the reactions occur spontaneously in triethylamine.

**Reaction mechanism and transition states.**

**Scheme 3.** 1,3-Dipolar cycloaddition of α-chlorobenzaldoxime and isatin.

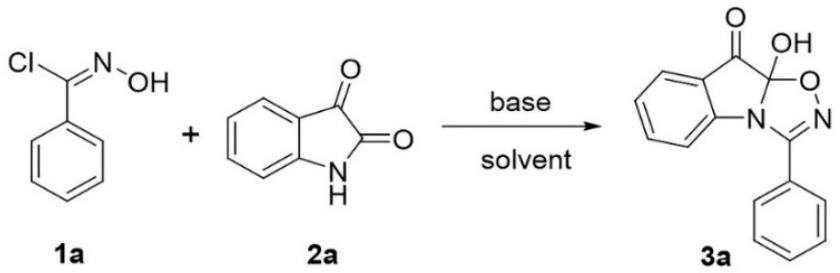


The reaction **1a** + **2a** - **3a** , shown in Scheme 3, was taken as an example. Optimization was carried out under gas- and liquid-phase conditions. The geometries of reactants **1a** and**2a** , intermediates **1a'** , **2a'** , med1, and med2, transition states TS1, TS2, and TS3, and end product **3a** were obtained.

**Study of the liquid-phase reaction mechanism.**

The Cartesian coordinates of the optimized structure of each stationary point in the liquid-phase reaction is provided in Supporting Information 4.

**Elementary reaction 1.**

First, chloroxime compound **1a** is activated in the presence of triethylamine to form the nitrile oxide intermediate, **1a'** , through transition state TS1. The geometry of each stationary point is shown in Figure 1.

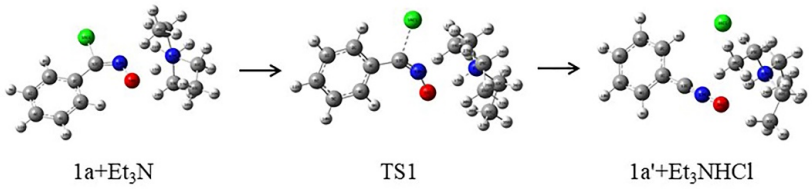


**Figure 1.** Geometries of the stationary points in the activation of **1a** to intermediate **1a'** by triethylamine.

The dihedral angle Cl(16)–C(12)–N(13)–O(14) in **1a** is coplanar. N(13) has a strong induced electron-withdrawing effect owing to its lone pair electrons, making the H atom of the hydroxyl group connected to it acidic. Through activation by the triethylamine solvent, a weak organic base, the hydroxyl H atom leaves **1a** . The triethylamine N atom provides a lone pair electron, while the H atom provides an empty orbital. The H atom migrates to triethylamine, resulting in an increase in the charge on the hydroxyl O atom. Because the C(12)–N(13) double bond is adjacent to the Cl atom, the C–Cl bond polarity is relatively high. The lone pair electrons on the N atom attack the C–N double bond, leading to sp hybridization and departure of the Cl atom carrying the negative charge. The C(12)–N(13) bond is gradually shortened from 1.283 to 1.161 Å and the N(13)–O(14) bond from 1.349 to 1.241 Å. The intermediate 1,3-dipole, **1a'** , which has a partial C–N double bond, is formed. The C(12)–N(13)–O(14) bond angle increases from 122.42° to 180.00°. The charge on the N atom decreases, while that on the O atom increases, and the molecule as a whole has no net charge.

Transition state TS1 was traced by IRC calculation, which confirmed that it is a first-order saddle point on the potential energy surface of the reaction. TS1 leads from **1a** to **1a'** , which is the reaction intermediate. The $\Delta E_{\ a}$ for this step is $\Delta E_{\ a1} = 22.1$ kcal·mol$^{-1}$. Using the energy of the product, [**1a'** +$Et_3NHCl$], as the reference, the energy level diagram of elementary reaction 1 was derived and is shown in Figure 2.

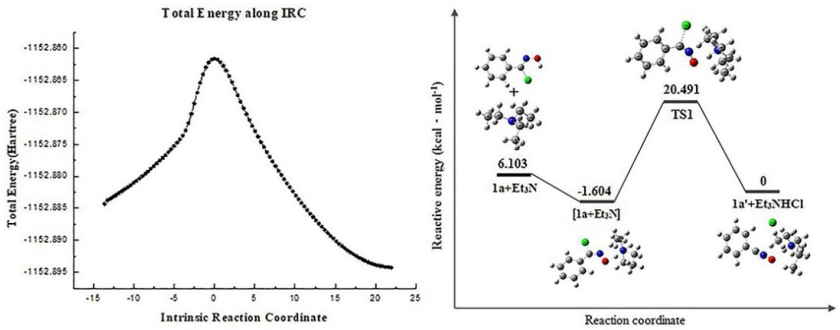


**Figure 2.** Intrinsic reaction coordinate (IRC) curve of TS1 and energy level diagram of elementary reaction 1.

Simultaneously, H(12) of isatin (**2a** ), which is connected to N(4), leaves in the presence of triethylamine, leading to an increase in the charge on N(4). The C(3)–O(11) bond length increases from 1.213 to 1.236 Å, while the N(4)–C(5) bond is shortened from 1.404 to 1.379 Å. The latter bond length is between that of a C–N single bond and C–N double bond; thus, N(4)–C(5) has a partial double bond character. The N(4)–C(3) bond is shortened from 1.380 to 1.358 Å, while the C(3)–N(4)–C(5) bond angle changes from 112.08° to 106.46°. The negative charge on N(4) increases when intermediate **2a'** , which has a net negative charge, is formed. Because of the strong electron-withdrawing effect of the carbonyl groups, the H atom on the amide is more acidic. It leaves more easily and bonds to the N atom of the weak organic base, triethylamine. This process occurs spontaneously without a transition state. The geometry of each stationary point is shown in Figure 3.

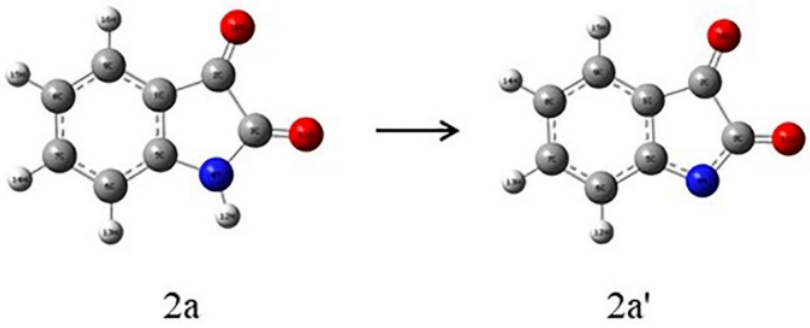


**Figure 3.** Geometries of the stationary points in the formation of anion intermediate **2a'** from isatin (**2a** ).

**Elementary reaction 2.**

Nucleophilic addition occurs between intermediates **1a'** and**2a'** . Electron-rich N(28) of **2a'** attacks C(6) of the dipole intermediate, **1a'** , leading to the formation of intermediate med1 through transition state TS2. The geometry of each stationary point is shown in Figure 4.

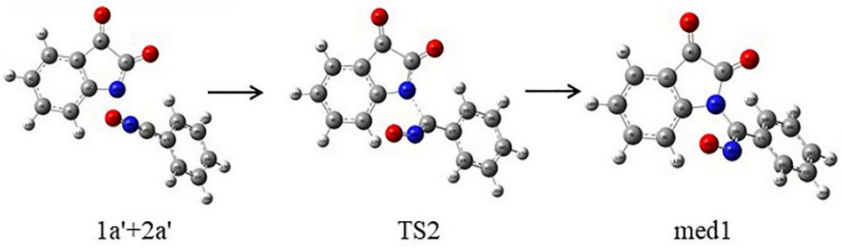


**Figure 4.** Geometries of the stationary points in the nucleophilic addition of intermediates **1a'** and **2a'** . Intermediate med1 is generated through transition state TS2.

During this reaction, the LUMO of **1a'** and HOMO of **2a'**are close to each other and their symmetries match, leading to an effective overlap, as shown in Figure 5.

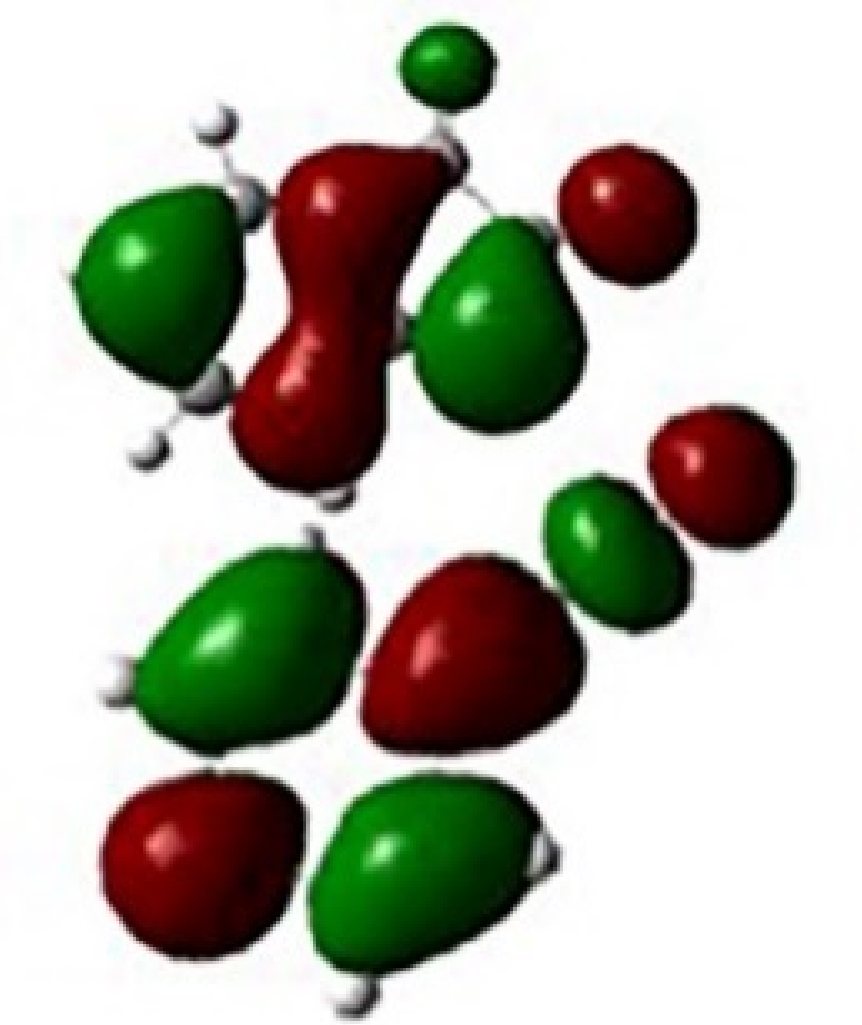

**Figure 5.** Overlapping lowest unoccupied molecular orbital of**1a'** and highest occupied molecular orbital

of **2a'** .

The benzene ring of **1a'** rotates, and the C(16)–N(28)–O(29) bond angle decreases gradually from 180.00°. C(6) of **1a'** and N(28) of **2a'** are close to each other, which facilitates their bonding. The reaction proceeds through transition state TS2 at which the C(16)–N(28) distance is 2.050 Å and the C(16)–N(28)–O(29) bond angle is 147.96°. Finally, the C(16)–N(28) single bond forms with a bond length of 1.432 Å and C(16)–N(28)–O(29) bond angle of 117.76°.

IRC calculation proved that TS2 is a first-order saddle point in the potential energy surface of the reaction. The $\Delta E$ $_{a}$for this step is $\Delta E$ $_{a2}$ = 9.76 kcal·mol$^{-1}$. For the IRC analysis of this process, different algorithms, including HPC, LQA and GS2, were adopted to obtain more accurate reactant and intermediate structures, and the number and size of steps were calculated. By comparison, it is concluded that when IRC is generated for the same transition state with the same step number and step size, LQA takes the shortest time, GS2 takes the second place, HPC takes the longest time, and the number of steps does not converge easily in the HPC algorithm. However, the use of LQA and GS2 algorithms can avoid such errors, because it does not involve the problem of correction step size. The HPC algorithm has the highest accuracy and yields more accurate reactants and products. The accuracy of GS2 is intermediate, while that of LQA is relatively poor. Figure 6 shows the IRC curve obtained by combining the *calcall* keyword (stepsize = 5, maxpoint = 200) with the HPC algorithm. With product **3a** as the reference, the energy level diagram of elementary reaction 2 was obtained and is shown in Figure 6.

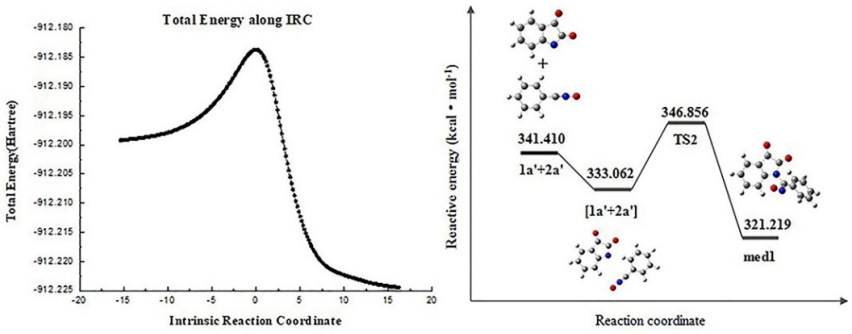


**Figure 6.** Intrinsic reaction coordinate (IRC) curve of TS2 and energy level diagram of elementary reaction 2.

**Elementary reaction 3.**

The intramolecular reaction of intermediate med1, which was formed by elementary reaction 2, can occur through the following two pathways.

Path 1: The electron-rich O atom of the nitroso group attacks the C atom on the Carbonyl directly, and intermediate med1 is cyclized through the five-membered transition state, TS3', to form intermediate med1-1. The electron-rich O(14) atom of med1-1 is then protonated in solution to form product **3a** , as shown in Figure 7.

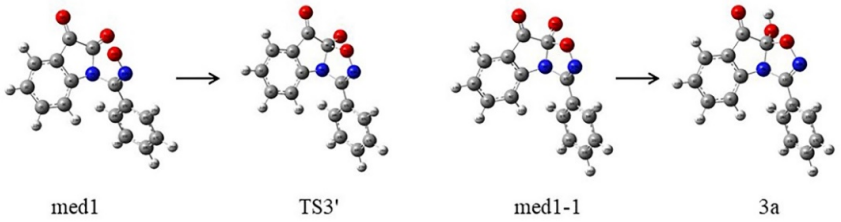


**Figure 7.** Geometries of the stationary points in the intramolecular reaction of intermediate med1 to form **3a** .

For path 1, we assumed that the $H^+$ in solution is not involved in the cyclization process. Although various configurations were tested, the transition state of this process was not found using either the ts, qst2, or qst3 method. The C(8)–O(14) bond length was scanned flexibly. The structural changes and energy curve during the scan are shown in Figures 8 and 9, respectively. The scan shows that as C(8) and O(14) become far away from each other, the energy of the system continuously increases without reaching the highest point in energy. When C(8) and O(14) are not bonded, the C(8)–N(7) bond is broken and a very unstable 8-membered ring system is formed. At the same time, after the structure of intermediate med1-1 is optimized, the C(8)–O(14) bond breaks and cannot form a stable five-membered ring, which proves that med1-1 is unstable under these conditions. Therefore, path 1 cannot occur, and it was hypothesized that $H^+$ participates in the formation of the five-membered ring.

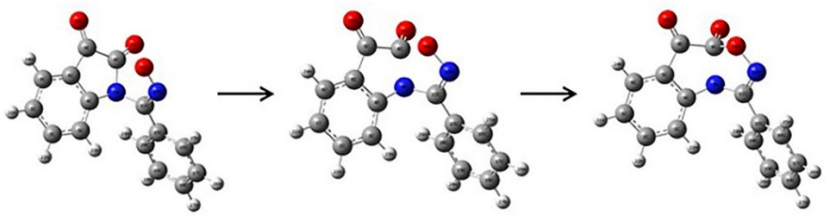

**Figure 8.** Geometries of the stationary points in the unassisted cyclization.

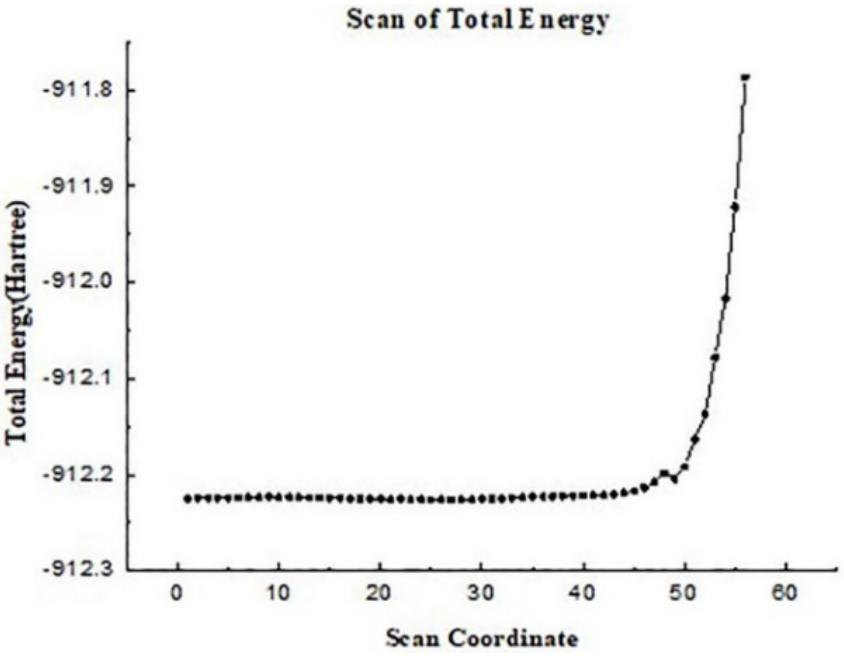


**Figure 9.** Flexible scan of the C(8)–O(14) bond.

Path 2: The $H^+$ in solution participates in the cyclization process and attacks electron-rich O(29), leading to protonation. Intramolecular hydrogen migration occurs after intermediate med1 is converted into med2 and the H atom migrates to the carbonyl O atom. Product **3a'** is formed through the five-membered transition state, TS3. The calculation and analysis show that this path is reasonable, and the geometries of the stationary points in the reaction are shown in Figure 10.

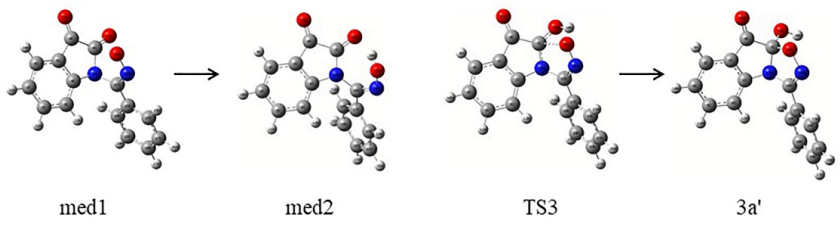


**Figure 10.** Geometries of the stationary points in $H^+$-assisted cyclization to generate product**3a'** .

During the reaction, the $H^+$ in solution migrates to O(29) to form intermediate med2, which was confirmed to be stable after geometry optimization. In theory, this process occurs spontaneously without a transition state. In med2, the N(13)–C(16)–N(28) bond angle is 124.88°, C(7) and O(29) are not bonded (bond distance of 2.940 Å), and the carbonyl C(7)–O(14) bond shows double bond character (bond length of 1.221 Å). As the reaction proceeds, C(7) and O(29) approach each other. The H atom bound to O(19) migrates to carbonyl O(14), and the C(7)–O(14) bond length increases to 1.316 Å. As the reaction crosses transition state TS3, the C(7)–O(14) bond length increases to 1.346 Å, and C(7) and O(29) forms a bond with a C(8)–C(7)–O(29) bond angle of 125.87°. As the molecule continues to rotate, the C(8)–C(7)–O(29) bond angle decreases to 113.11° and the configurational energy continues to decrease, resulting in the formation of **3a'** . In **3a'** , the N(13)–C(16)–N(28) bond angle is 113.29°, the C(7)–O(29) bond length is 1.431 Å, and the carbonyl C(7)–O(14) bond length is 1.378 Å.

Transition state TS3 was traced by IRC calculation, which proved that it is a first-order saddle point in the potential energy surface of the reaction. The $\Delta E_{\ a}$ for this process is $\Delta E_{\ a3} = 26.92$ kcal·mol$^{-1}$. With product **3a** as the reference, the energy level diagram of elementary reaction 3 was calculated and is shown in Figure 11.

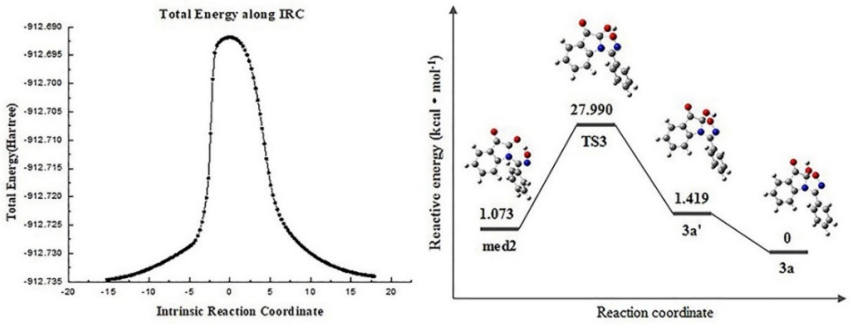


**Figure 11.** Intrinsic reaction coordinate (IRC) curve of TS3 and energy level diagram of elementary reaction 3.

From the structure, it can be seen that H(30) of **3a'** rotated. As shown in Figure 13, the dihedral angle C(8)–C(7)–O(14)–H(30) was flexibly scanned in 360 steps with a step length of 1°. Configuration $3a_0$ of the product has the lowest energy and was further optimized to obtain the final product, **3a** . The geometries of the stationary points are shown in Figure 12.

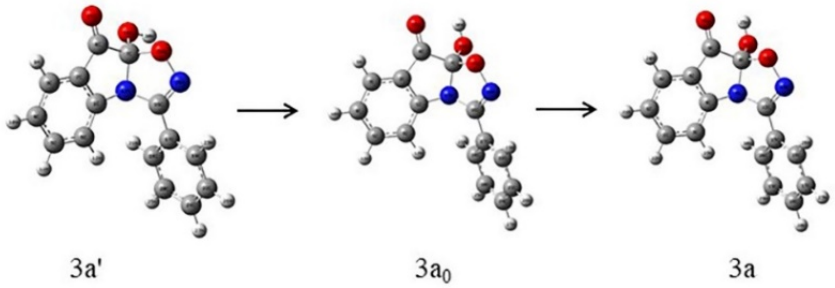


**Figure 12.** Geometries of the stationary points after optimization of the **3a'** structure.

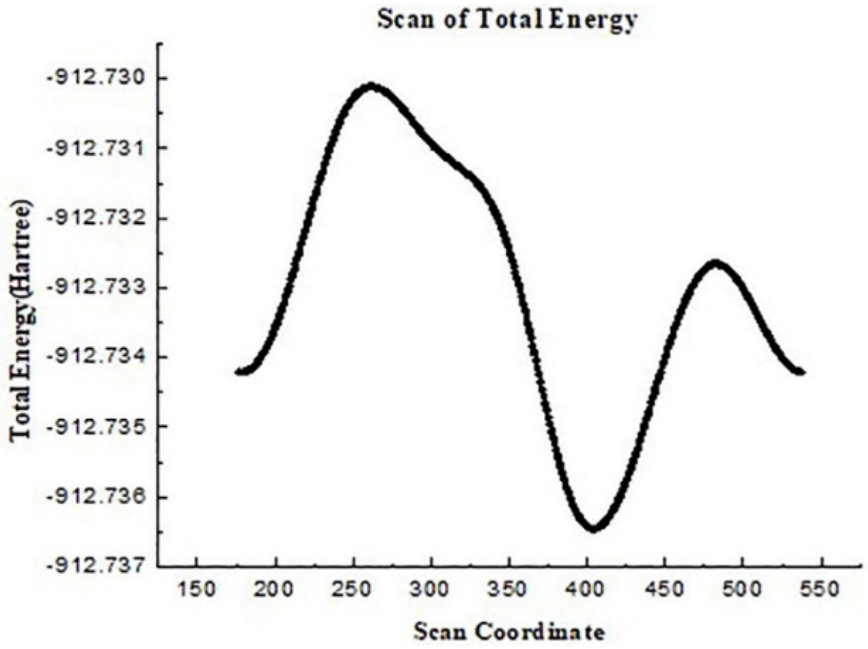


**Figure 13.** Flexible scan of the C(8)–C(7)–O(14)–H(30) dihedral.

**Study of the gas-phase reaction mechanism.**

The biggest difference between the gas- and liquid-phase reactions is that there are solvent molecules in the latter. For the same reaction, there are different reaction rates and likely different reaction processes. This is because the dielectric constant, polarity, ionic strength, and solvation have different effects on the reaction rate. For the system we studied, the solvent molecules themselves are involved in the reaction. Therefore, the reaction mechanism under the gas-phase condition is discussed, and the similarities and differences from the solution-phase condition were analyzed.

For elementary reactions 1–3, the gas-phase reaction follows the same reaction paths as the liquid-phase reaction. Intermediates**1a'** _gas, **2a'** _gas, med1_gas, and med2_gas, were formed during the reaction, as well as transition states TS1_gas, TS2_gas, and TS3_gas. The optimized structures of the stationary points are basically similar, as shown in Figure 14.

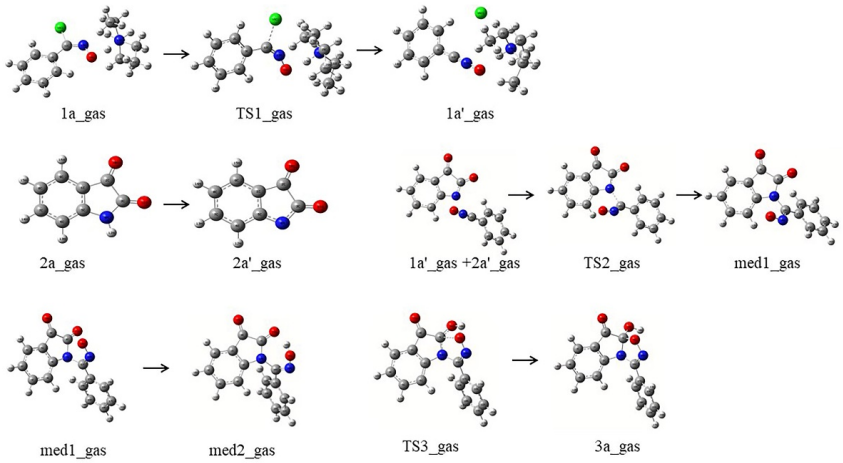

**Figure 14.** Geometries of intermediates and transition states in elementary reactions 1–3 in the gas phase.

In elementary reaction 3, $H^+$ ions are also needed to form the five-membered ring; otherwise, a stable intermediate cannot be formed. For the two-step elementary reaction, the $\Delta E_a$ values in the gas- and liquid-phase environments are shown in Table 13. When the reaction is carried out in a gas-phase environment, the reactant molecules can collide directly without resistance. In the triethylamine solvent, the reactant molecules are solvated, which hinders the effective collision of the molecules. It can be inferred from the discussion in section 3.1 that the system is less affected by the polar triethylamine solvent. On the other hand, in elementary reaction 3, triethylamine has an attractive effect on the $H^+$ ions in solution. According to a comprehensive comparison, for elementary reactions 2 and 3, the $\Delta E_a$ values in the solvent phase are slightly higher than those in the gas phase. However, in elementary reaction 1, there is no triethylamine solvent, and the $\Delta E_a$for forming intermediates **1a'** and **2a'** from reactants**1a** and **2a** , respectively, is higher.

**Table 3.** Activation energies ($\Delta E_a$) of each reaction step in the liquid and gas phases.

| $\Delta E_\alpha$ (кслал·молл$^{-1}$) Condition | Elementary reaction 1 | Elementary reaction 2 | Elementary reaction 3 |
|---|---|---|---|
| **Liquid phase with triethylamine as solvent** | 22.1 | 9.8 | 26.9 |
| **Gas phase** | 27.7 | 9.4 | 26.4 |

**Comparison of the $\Delta E_a$ of different reactions.**

For the whole reaction process, there are three elementary reactions and three transition states. The removal of $H^+$ and $Cl^-$ from reactant **1a** through transition state TS1 is carried out in triethylamine solvent. The cyclization of intermediate med2 to **3a** through transition state TS3 is an intramolecular reaction. On the other hand, the reaction between intermediates **1a'** and **2a'** to form intermediate med1 through transition state TS2 is an intermolecular reaction that is greatly affected by a substituent. Therefore, elementary reaction 2 was further investigated by selecting reactants with different substituents.

Because the reaction is LUMO controlled, changing the substituent on reactant **1a** has a greater effect. The reactions (elementary reaction 2) of **1a** , **1b** , **1f** , **1g** ,**1j** , **1m** , **1n** , and **1o** with **2a**were studied. Reactants **1a** , **1b** , **1f** ,**1g** , **1j** , and **1m** contain a phenyl group with H, $CH_3$, $OCH_3$, F, Cl, and Br substituents, respectively. On the other hand, **1n** is thiophene substituted and **1o** is alkyl substituted. The molecular configurations of the reactants and products were optimized, and IRC tracing was carried out. The calculation shows that the reaction path of dienophile**1a** does not change whether the substituent is an electron-donating or electron-withdrawing group. Figures 15(a–h) shows the IRC curves for the different substituted reactants.

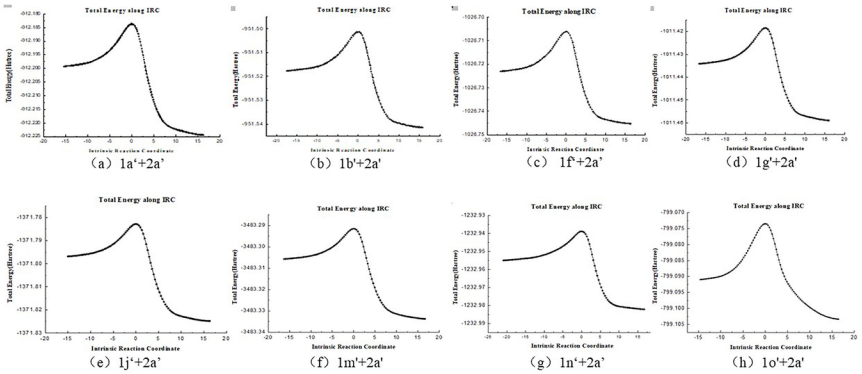

**Figure 15.** Intrinsic reaction coordinate (IRC) curves for the different substituted reactants.

As can be seen in Table 14, for reactant **1a** substituted with phenyl, thiophene, and alkyl groups, the required $\Delta E_{\ a}$, i.e., degree of difficulty, for elementary reaction 2 increases in the order Ph < thiophene < n-Pr. Thus, a conjugated ring system is more favorable for the reaction. The C atoms on the benzene ring are hybridized to provide 2p orbitals in the $sp^2$ mode, while the S atom in thiophene is conjugated with the 3p orbital electrons. The overlap of orbitals is slightly worse because the radius of a 3p orbital is larger than that of a 2p orbital. Consequently, the conjugation effect of thiophene is not as good as that of benzene.

For substituted benzene, electron-withdrawing groups, such as F, Cl, and Br, are more conducive to the reaction because they lower the $\Delta E_{\ a}$. Among the substituted reactants, the $\Delta E_{\ a}$ for the F-substituted reactant is slightly higher than those of the Cl- and Br-substituted reactants because the induced electron-withdrawing effect of F, which is a conjugate electron donor, is weaker. Substitution with $CH_3$, $OCH_3$, or other electron-donating groups lead to a higher $\Delta E_{\ a}$, that is, an electron-donating group is not conducive to the reaction.

**Table 4.** Activation energies ($\Delta E_{\ a}$) for different substituted compounds.

| Substituent | | | | | | | | |
|---|---|---|---|---|---|---|---|---|
| $\Delta E_a$ (kcal·mol$^{-1}$) | 9.8 | 10.3 | 10.6 | 9.8 | 8.8 | 8.9 | 10.2 | 11.0 |

## Conclusions

In conclusion, this study takes advantage of our previous work on 1,3-dipolar cycloaddition where we synthesized 36 novel polyheterocyclic 1,2,4-oxadiazolindolone compounds by a one-step reaction.[31] The 6-31G(d) basis set and B3LYP, M052X, M062X, and APFD functionals were used to optimize the geometries and determine the vibrational frequencies of 5 reactants, 5 intermediates, and 36 products. The results showed symmetry matching between the LUMO of substituted chloroxime compounds and HOMO of substituted isatin in the LUMO-controlled reaction. Furthermore, the presence of a phenyl group in chloroxime is more conducive to the reaction because an electron-withdrawing substituent on the phenyl group can reduce the LUMO energy level of the reactant and thus facilitate the reaction. When isatin is substituted with an electron-donating group, the HOMO energy level increases, which is also beneficial to the reaction. In this study, the applicability of the B3LYP functional to this system was determined, and the reaction mechanism was discussed at the B3LYP/6-31G(d) level. The three main elementary reactions and corresponding transition states, TS1, TS2, and TS3, in the liquid and gas phases were calculated and discussed. Using the IRC method, the accuracy of the transition states was confirmed, and the advantages and disadvantages of LQA, HPC, and GS2 in producing the IRC were compared. HPC produced an IRC curve with higher accuracy, and the two ends of the curve were closer to the structure of the product. The reaction process was calculated. Finally, by comparing the $\Delta E_{\ a}$values for the gas- and liquid-phase reactions, it was proven that the solvent only has a minor effect on the reaction process. This study is expected to have a long-term significance by providing useful ideas for the design of more effective drugs of this kind in the future.

ASSOCIATED CONTENT

**Supporting Information** .

The following files are available free of charge.

The specific experimental steps, the energy difference between the lowest unoccupied molecular orbital (LUMOs) and the highest occupied molecular orbital (HOMOs) of the reactants at different levels, the ΔG of each reaction in the gas phase at different levels. And the Cartesian coordinates (Å) of the optimal structure of the fixed point in the liquid phase reaction can be seen in the attachment support information. (file type, i.e., PDF)

Notes

The authors declare no competing financial interest.

**Acknowledgment**

We would like to thank the National Natural Science Foundation of China (Grant Nos. 21465025 and 81860623) for financial support of this work, as well as the High Performance Computing Center of Yunnan University for providing computing resources and Information Technology Center of Yunnan University for providing technical support.

**References**

1. Yen-Pon, E.; Champagne, P. A.; Plougastel, L.; Gabillet, S.; Thuery, P.; Johnson, M.; Muller, G.; Pieters, G.; Taran, F.; Houk, K. N.; Audisio, D., Sydnone-Based Approach to Heterohelicenes through 1,3-Dipolar-Cycloadditions. *J Am Chem Soc* **2019,***141* (4), 1435-1440.

2. Gracia-Vitoria, J.; Osante, I.; Cativiela, C.; Tejero, T.; Merino, P., Experimental and Computational Studies on the 1,3-Dipolar Cycloaddition between Enantiomerically Pure 2,3-Dihydrothiazoles and Nitrones. *Eur J Org Chem* **2019,** *2019* (27), 4426-4435.

3. Ren, D.; Hu, X.; Li, X., Synthesis of novel dispiro[indoline-3,2'-pyrrolidine-3',10"-thiazolo[3',2':1,2]pyrimido[5,4-g]indolizine] derivatives by 1,3-dipolar cycloaddition reaction. *Chemistry of Heterocyclic Compounds* **2019,** *55* (3), 275-279.

4. Arhin, G.; Adams, A. H.; Opoku, E.; Tia, R.; Adei, E., 1, 3-Dipolar cycloaddition reactions of selected 1,3-dipoles with 7-isopropylidenenorbornadiene and follow-up thermolytic cleavage: A computational study. *J Mol Graph Model* **2019,** *92* , 267-279.

5. Yue, J.; Chen, S.; Zuo, X.; Liu, X.-L.; Xu, S.-W.; Zhou, Y., Diversity-oriented one-pot multicomponent synthesis of chromanone-based 3,3'-pyrrolidinyl-spirooxindoles via a 1,3-dipolar cycloaddition reaction. *Tetrahedron Letters* **2019,** *60* (2), 137-141.

6. Mortensen, K. T.; Osberger, T. J.; King, T. A.; Sore, H. F.; Spring, D. R., Strategies for the Diversity-Oriented Synthesis of Macrocycles.*Chem Rev* **2019,** *119* (17), 10288-10317.

7. Burke, M. D.; Schreiber, S. L., A planning strategy for diversity-oriented synthesis. *Angew Chem Int Ed Engl***2004,** *43* (1), 46-58.

8. Schreiber, S., Target-Oriented and Diversity-Oriented Organic Synthesis in Drug Discovery. *Science* **2000,** *287* ( 5460), 1964-1969.

9. Arya, P.; Joseph, R.; Gan, Z.; Rakic, B., Exploring new chemical space by stereocontrolled diversity-oriented synthesis. *Chem Biol***2005,** *12* (2), 163-180.

10. Lu, T.; Wang, C.; Wang, G.; Wang, S.; Song, J.; Yin, H.; Fan, G.; Chen, F.-X., 1,2,4-Oxadiazole-derived polynitro energetic compounds with sensitivity reduced by a methylene bridge. *New Journal of Chemistry* **2019,** *43* (34), 13330-13333.

11. Chiacchio, M. A.; Legnani, L.; Campisi, A.; Paola, B.; Giuseppe, L.; Iannazzo, D.; Veltri, L.; Giofre, S.; Romeo, R., 1,2,4-Oxadiazole-5-ones as analogues of tamoxifen: synthesis and biological evaluation.*Org Biomol Chem* **2019,** *17* (19), 4892-4905.

12. Srinivas, M.; Satyaveni, S.; Ram, B., Synthesis and Anticancer Activity of 1,2,4-Oxadiazol Linked Benzimidazole Derivatives.*Russian Journal of General Chemistry* **2019,** *88*(12), 2653-2657.

13. Kumar, D.; Patel, G.; Vijayakrishnan, L.; Dastidar, S. G.; Ray, A., Design and synthesis of 3,5-disubstituted-1,2,4-oxadiazoles as potent inhibitors of phosphodiesterase4b2. *Chem Biol Drug Des***2012,** *79* (5), 810-818.

14. Cottrell, D. M.; Capers, J.; Salem, M. M.; DeLuca-Fradley, K.; Croft, S. L.; Werbovetz, K. A., Antikinetoplastid activity of 3-aryl-5-thiocyanatomethyl-1,2,4-oxadiazoles. *Bioorg Med Chem***2004,** *12* (11), 2815-2824.

15. Miralinaghi, P.; Salimi, M.; Amirhamzeh, A.; Norouzi, M.; Kandelousi, H. M.; Shafiee, A.; Amini, M., Synthesis, molecular docking study, and anticancer activity of triaryl-1,2,4-oxadiazole.*Medicinal Chemistry Research* **2013,** *22* (9), 4253-4262.

16. Gakh, A. A.; Sosnov, A. V.; Krasavin, M.; Nguyen, T. L.; Hamel, E., Identification of diaryl 5-amino-1,2,4-oxadiazoles as tubulin inhibitors: the special case of 3-(2-fluorophenyl)-5-(4-methoxyphenyl)amino-1,2,4-oxadiazole.*Bioorg Med Chem Lett* **2013,** *23* (5), 1262-1268.

17. Muraglia, E.; Ontoria, J. M.; Branca, D.; Dessole, G.; Bresciani, A.; Fonsi, M.; Giuliano, C.; Llauger Bufi, L.; Monteagudo, E.; Palumbi, M. C.; Torrisi, C.; Rowley, M.; Steinkuhler, C.; Jones, P., N-(2-alkylaminoethyl)-4-(1,2,4-oxadiazol-5-yl)piperazine-1-carboxamides as highly potent smoothened antagonists. *Bioorg Med Chem Lett***2011,** *21* (18), 5283-5288.

18. Carette, X.; Blondiaux, N.; Willery, E.; Hoos, S.; Lecat-Guillet, N.; Lens, Z.; Wohlkonig, A.; Wintjens, R.; Soror, S. H.; Frenois, F.; Dirie, B.; Villeret, V.; England, P.; Lippens, G.; Deprez, B.; Locht, C.; Willand, N.; Baulard, A. R., Structural activation of the transcriptional repressor EthR from Mycobacterium tuberculosis by single amino acid change mimicking natural and synthetic ligands. *Nucleic Acids Res* **2012,** *40* (7), 3018-3030.

19. Flipo, M.; Desroses, M.; Lecat-Guillet, N.; Villemagne, B.; Blondiaux, N.; Leroux, F.; Piveteau, C.; Mathys, V.; Flament, M. P.; Siepmann, J.; Villeret, V.; Wohlkonig, A.; Wintjens, R.; Soror, S. H.; Christophe, T.; Jeon, H. K.; Locht, C.; Brodin, P.; Deprez, B.; Baulard, A. R.; Willand, N., Ethionamide boosters. 2. Combining bioisosteric replacement and structure-based drug design to solve pharmacokinetic issues in a series of potent 1,2,4-oxadiazole EthR inhibitors. *J Med Chem* **2012,** *55* (1), 68-83.

20. Nakamura, A.; Kaneko, N.; Villemagne, V. L.; Kato, T.; Doecke, J.; Dore, V.; Fowler, C.; Li, Q. X.; Martins, R.; Rowe, C.; Tomita, T.; Matsuzaki, K.; Ishii, K.; Ishii, K.; Arahata, Y.; Iwamoto, S.; Ito, K.; Tanaka, K.; Masters, C. L.; Yanagisawa, K., High performance plasma amyloid-beta biomarkers for Alzheimer's disease. *Nature***2018,** *554* (7691), 249-254.

21. Senthil Periyasmay; Subbiah, S., Modifications to the process for the synthesis of new 1,2,4-oxadiazole analogues and the short review on synthetic methodologies of 1,2,4oxadiazoles. *International Journal of Life Sciences Research* **2019,** *7* (2), 87-104.

22. Jiang, C. S.; Fu, Y.; Zhang, L.; Gong, J. X.; Wang, Z. Z.; Xiao, W.; Zhang, H. Y.; Guo, Y. W., Synthesis and biological evaluation of novel marine-derived indole-based 1,2,4-oxadiazoles derivatives as multifunctional neuroprotective agents. *Bioorg Med Chem Lett***2015,** *25* (2), 216-220.

23. Kumpuga, B. T.; Itsuno, S., Synthesis of chiral polyesters of cinchona alkaloid catalysts for enantioselective Michael addition of anthrone to nitroalkenes. *Journal of Catalysis* **2018,***361* , 398-406.

24. Nehal Ibrahim; Hany Ibrahim; Sothea Kim; Jean-Pierre Nallet; Nepveu, F. o., Interactions between Antimalarial Indolone-N-oxide Derivatives and Human Serum Albumin. *Biomacromolecules* **2010,***11* (12), 3341-3351

25. Porter, J. D.; Vivas-Rodriguez, O. L.; Weaver, C. D.; Dickson, E. J.; Alsafran, A.; DiMilo, E.; Arnold, L. A.; Dockendorff, C., An anthrone-based Kv7.2/7.3 channel blocker with improved properties for the investigation of psychiatric and neurodegenerative disorders.*Bioorganic & Medicinal Chemistry Letters* **2019,***126681* .

26. Cheng, C.; Li, Z.; Shu, J.; Li, T.; Zhang, B., Synthesis of isoxazolidines by 1,3-dipolar cycloaddition and their bioactivity.*Frontiers of Chemistry in China* **2006,** *1* (4), 427-433.

27. Norman, M.; Minick, D.; Rigdon, G., Effect of linking bridge modifications on the antipsychotic profile of some phthalimide and isoindolillone derivatives. *Journal Of Medicinal Chemistry***1996,** *39* (1), 149-157.

28. Pansare, S. V.; Lingampally; Rajinikanth; Kirby; Raie Lene, Stereoselective Synthesis of 3-Aryloctahydroindoles and Application in a Formal Synthesis of (-)-Pancracine. *Organic Letters***2010,** *12* (3), 556-559

29. Miles, C.; Trehy, M.; Yost, R., Degradation Of N-Methylcarbamate and Carbamoyl Oxime Pesticides In Chlorinated Water. *Bulletin Of Environmental Contamination and Toxicology* **1988,** *41*(6), 838-843.

30. Frisch, M.; Clemente, F., Gaussian 09, Revision A. 01, MJ Frisch, GW Trucks, HB Schlegel, GE Scuseria, MA Robb, JR Cheeseman, G.*Scalmani, V. Barone, B. Mennucci, GA Petersson, H. Nakatsuji, M. Caricato, X. Li, HP Hratchian, AF Izmaylov, J. Bloino, G. Zhe* .

31. Jiang, K. M.; Luesakul, U.; Zhao, S. Y.; An, K.; Muangsin, N.; Neamati, N.; Jin, Y.; Lin, J., Tautomeric-Dependent Lactam Cycloaddition with Nitrile Oxide: Facile Synthesis of 1,2,4-Oxadiazole[4,5-a]indolone Derivatives. *ACS Omega***2017,** *2* (7), 3123-3134.

32. Fukui, K.; Yonezawa, T.; Nagata, C.; Shingu, H., Molecular Orbital Theory of Orientation in Aromatic, Heteroaromatic, and Other Conjugated Molecules. *The Journal of Chemical Physics* **1954,***22* (8), 1433-1442.